# Intelligent Tracking of Network Dynamics for Cross-Technology Coexistence Over Unlicensed Bands

Mohammed Hirzallah<sup>1</sup>, Marwan Krunz<sup>1,2</sup>

<sup>1</sup>Department of Electrical and Computer Engineering, University of Arizona, AZ, USA <sup>2</sup>School of Electrical and Data Engineering, University of Technology Sydney, NSW, Australia Email: {hirzallah, krunz}@email.arizona.edu

Abstract—Unlicensed bands offer great opportunities for numerous wireless technologies, including IEEE 802.11-based systems, 4G Licensed-Assisted-Access (LAA), and 5G New Radio Unlicensed (NR-U) networks. Achieving harmonious coexistence between these technologies requires real-time adaptation of their channel access, which can be facilitated by artificial intelligence (AI) and machine learning (ML) techniques. However, to leverage such techniques, we need to characterize the state of unlicensed wireless channel and the dynamics of the coexisting systems. In this paper, we introduce the concept of Sensing Fingerprint (SF) profile to characterize the state of coexisting networks and track their dynamics over unlicensed bands. We conduct extensive experiments to show the effectiveness of SF profile in tracking key network dynamics, including sensitivity thresholds of contending devices, their mobility, traffic loads, and other channel access parameters. AI- and ML-based controllers can utilize this tool to model the state of coexisting networks and track their dynamics.

Index Terms—Feature selection and extraction, intelligent tracking, machine learning, cross-technology coexistence, 5G New Radio Unlicensed (NR-U), LAA, IEEE 802.11.

## I. INTRODUCTION

Unlicensed spectrum below 7 GHz supports a variety of heterogeneous wireless technologies, including IEEE 802.11based Wi-Fi systems, 4G Licensed-Assisted-Access (LAA), and 5G New Radio Unlicensed (NR-U) [1][2][3]. In particular, NR-U/LAA will enable mobile network operators (MNOs) to increase their data rates by aggregating their licensed carriers with unlicensed ones. The standalone version of NR-U also offers a great opportunity for new MNOs that do not own licensed spectrum to launch new services over unlicensed bands. Coexistence between these technologies gives rise to many challenges, including fairness and cross-technology interference [4]. To access an unlicensed channel in the 5-7 GHz bands, devices rely on Listen-Before-Talk (LBT) procedure whereby each contending device measures the received signal and compares it with a predetermined threshold, a.k.a., sensitivity threshold (ST), to determine the channel is idle. In executing the LBT procedure, Wi-Fi/LAA/NR-U devices could adopt different channel access parameters and rely on different STs, and, consequently, resulting in being unfair to each other.

This research was supported in part by NSF and by the Broadband Wireless Access & Applications Center (BWAC). Any opinions, findings, conclusions, or recommendations expressed in this paper are those of the author(s) and do not necessarily reflect the views of NSF.

To achieve fair access to unlicensed channels and harmonious coexistence among Wi-Fi and NR-U systems, many operational parameters, such as the LBT parameters and STs, need to be adapted in real-time. Artificial intelligence (AI) and machine learning (ML) algorithms can play a significant role in this adaptation, but they still require proper features and measurements to characterize the wireless environment and track the dynamics of the coexisting systems.

To obtain a proper feature representation of the wireless channel, we conduct extensive system-level simulations, based on our customized C++-based discrete-event simulator, to allow us to understand how NR-U and Wi-Fi throughputs change as function of their network dynamics, including mobility, traffic loads, and channel access parameters (STs and LBT parameters). The concept of *Sensing Fingerprint (SF) profile* is defined to characterize the state of NR-U and Wi-Fi networks and track their dynamics. We demonstrate the effectiveness of SF profile as a powerful tool for supporting AI-/ML-based algorithms that can track the state of the wireless environment. The SF profile is shown to have a strong correlation with different channel access parameters as well as the dynamics of coexisting systems.

To signal changes in network dynamics, we explore various statistical metrics whereby we evaluate the divergence between SF profiles captured over different times and under different scenarios. We evaluate the variance in divergence for the considered metrics, including the normalized difference in mean, normalized difference in variance, difference in energy, Kullback-Liebler, Jensen-Shannon, Hellinger distance, and Bhattacharayya distance, and find that the Kullback-Liebler divergence measure and Hellinger distance are the best metrics to signal changes of vital network dynamics, when applied to SF profile.

The rest of the paper is organized as follows. In Section II, we give a background on LBT and STs adopted in NR-U and Wi-Fi. We present our system model in Section III, and investigate how NR-U and Wi-Fi throughputs change as a function of different network dynamics in Section IV. In Section V, we introduce the SF profile. We evaluate different divergence measures in Section VI, and review related works in Section VII.

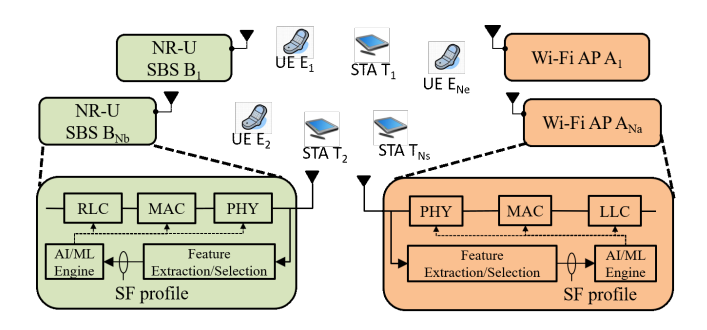


Fig. 1. System model (we focus on the design of the 'Feature Extraction/Selection' blocks).

### II. BACKGROUND

IEEE 802.11-based systems and NR-U rely on different variants of the Carrier Sense Multiple Access with Collision Avoidance (CSMA/CA) procedure, commonly known as LBT, to access unlicensed channels. In CSMA/CA with exponential backoff, if the channel remains idle for a certain period of time, called Arbitration Inter-Frame Space (AIFS) (or Initial Deferment period in NR-U), the device can start its transmission. Let  $\rho$  be the AIFS duration. To detect whether the channel is idle or not, the device compares the received signal with a predefined ST. If the channel becomes busy during the AIFS the device backs off for k idle timeslots, where:

$$k \in \{0, \cdots, \min\{2^j W_{\min}, W_{\max}\} - 1\}$$
 (1)

where  $W_{\min}$  and  $W_{\max}$  are the minimum and maximum backoff durations, and j is the retransmission attempt (j = $0, 1, \cdots$ ). The device freezes the backoff counter if the channel becomes busy and resumes counting down when channel becomes idle again. Transmission commences once the counter reaches zero. The effective throughput highly depends on the adopted LBT parameters and the ST value. Wireless technologies operating over unlicensed bands adopt different settings for their STs. LAA and NR-U specifications rely on an energybased ST of -72 dBm [5], whereas IEEE 802.11n/ac standards implement two STs, one that is based on energy detection (= -62 dBm) while the other is based on signal/preamble detection, i.e., waveform-based detection (= -82 dBm) [6]. In IEEE 802.11ax/be drafts, devices are expected to adapt their signal-based STs to improve the spectrum reuse between overlapping networks [7].

# III. System Model

We consider a coexistence scenario where a 5G NR-U network shares an arbitrary unlicensed channel with a Wi-Fi network, as shown in Figure 1. The NR-U network consists of a set  $\mathcal{B}=\{B_1,B_2,\cdots,B_{N_b}\}$  of  $N_b$  small-cell base stations (SBSs) that serve a set  $\mathcal{E}=\{E_1,E_2,\cdots,E_{N_e}\}$  of  $N_e$  user equipments (UEs). The Wi-Fi network consists of a set  $\mathcal{A}=\{A_1,A_2,\cdots,A_{N_a}\}$  of  $N_a$  access points (APs) that serve a set  $\mathcal{T}=\{T_1,T_2,\cdots,T_{N_s}\}$  of  $N_s$  stations (STAs). Let  $\alpha^{(u)}$  be the ST adopted by NR-U devices, and  $\alpha^{(w)}$  be the ST adopted by Wi-Fi devices. We consider different values for

 $\alpha^{(u)}$  and  $\alpha^{(w)}$ , including these adopted by the standards. Let  $W_{\min}^{(u)}, W_{\max}^{(u)}$ , and  $\rho^{(u)}$  be the minimum/maximum contention window and AIFS parameters used in NR-U network, and let  $W_{\min}^{(w)}, W_{\max}^{(w)}$ , and  $\rho^{(w)}$  be their counterpart used in the Wi-Fi network. NR-U and Wi-Fi devices generate a Poisson traffic. Let  $\pi_i^{(u)}$  be the traffic intensity of NR-U device i, and  $\pi_i^{(w)}$  be the traffic intensity of Wi-Fi device i. We consider a discrete time with a slot duration  $\tau$  that corresponds to the duration of a MAC time slot. For instance,  $\tau$  is set to 9 microseconds in NR-U specifications and IEEE 802.11 standards operating over the 5 GHz UNII bands [8][6]. Let  $\vartheta_i^{(u)}(n)$  be indicator function of NR-U device i to access the channel at an arbitrary time slot n, and  $\vartheta_i^{(w)}(n)$  be indicator function of Wi-Fi device i to access the channel at an arbitrary time slot n. There are many factors that affect the setting of these indicator functions at a specific time instant, including mobility, traffic loads, and channel access parameters. Formulation of these indicator functions requires notoriously complicated stochastic geometry analysis and depends on network topology [9]. Let  $y_i^{(u)}(n)$  be the received signal strength by an NR-U device, say i, at time n.  $y_i^{(u)}(n)$  can be expressed as (similar expressions can be formulated for Wi-Fi devices):

$$y_i^{(u)}(n) = \sum_{j \in \mathcal{B} \cup \mathcal{E}, j \neq i} P_j \Lambda_{ji} \vartheta_j^{(u)}(n) + \sum_{k \in \mathcal{A} \cup \mathcal{T}} P_k \Lambda_{ki} \vartheta_k^{(w)}(n)$$
(2)

where  $P_j$  is the transmit power of an arbitrary device j,  $\Lambda_{ji}$  is the channel loss between two arbitrary devices j and i (including path losses, shadowing, and fading). In this paper, we focus on the design for the 'Feature extraction/selection' blocks shown in Figure 1.

# IV. OPTIMAL SETTING OF CHANNEL ACCESS PARAMETERS

As observed in Equation (2), the received signal strength y(n) depends on many factors, including the STs and LBT parameters adopted by the two coexisting technologies. Unfortunately, formulating the effective throughput as a function of these channel access parameters is notoriously complicated. Therefore, we conduct system-level-based simulation experiments to investigate how NR-U and Wi-Fi channel access parameters need to be set with respect to other network parameters to achieve optimal NR-U and/or Wi-Fi performance. Due to space limit, we focus on the setting of sensitivity thresholds. We consider an NR-U network of three BSs that serve 15 UEs. The Wi-Fi network has three APs that serve 15 STAs. Initially, we consider a fixed topology and vary the STs for NR-U and Wi-Fi devices with fixed transmission rates (i.e., Wi-Fi: BPSK with 1/2 code rate, NR-U: OPSK with 1/5 code rate), as shown in Figure 2(a). We plot the downlink network throughput versus STs of NR-U and Wi-Fi networks. NR-U and Wi-Fi networks have multiple local optima. Adapting STs to achieve one of these local optima might require cooperation/competition between the two networks until they reach an equilibrium point.

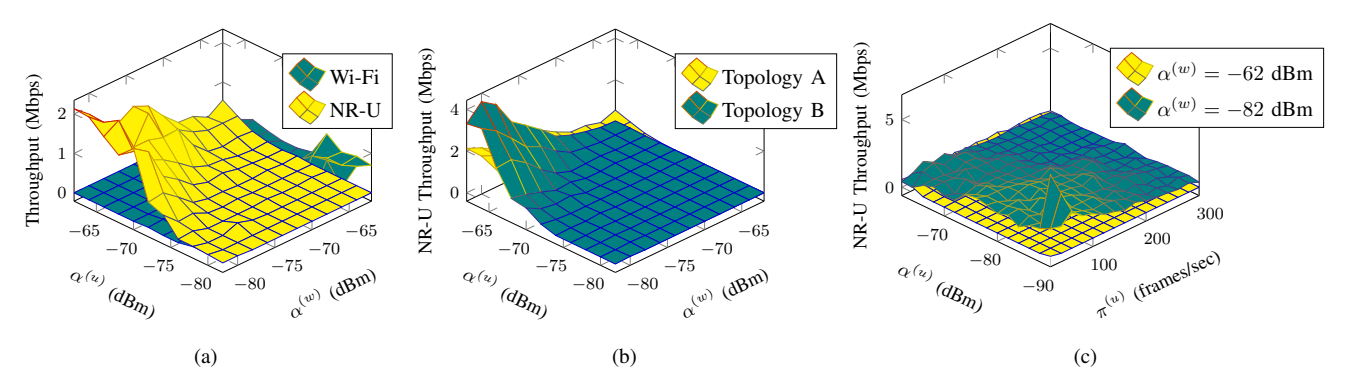


Fig. 2. (a) Downlink throughput vs. NR-U and Wi-Fi STs, (b) NR-U throughput vs. NR-U and Wi-Fi STs for two different topologies, and (c) NR-U throughput vs. ST and traffic load of NR-U for two different ST settings of Wi-Fi.

We study the impact of mobility on the optimal setting of NR-U and Wi-Fi STs by letting UEs and STAs move in a random walk fashion for 10 seconds. We plot the NR-U throughput versus STs of NR-U and Wi-Fi before (Topology A) and after devices start moving (Topology B), as shown in Figure 2(b). The optimal value of NR-U throughput changes due to mobility. The coexisting networks need to be aware of the mobility of the coexisting devices to properly adapt their STs. We also investigate the impact of traffic intensity and ST setting on NR-U throughput under different Wi-Fi ST settings, as shown in Figure 2(c). For a given traffic intensity, the setting of NR-U ST could achieve different throughput based on the ST setting adopted by Wi-Fi. We obtained similar results for Wi-Fi but we omit them due to space limitation. The above experiments reveal how it is difficult to achieve an optimal and fair setting of channel access parameters for NR-U and Wi-Fi systems.

# V. PROFILE OF SENSING FINGERPRINT (SF)

As it is observed from the previous section, to select fair and optimal channel access parameters of NR-U and Wi-Fi technologies, we need a global knowledge about the dynamics of the coexisting networks, including their mobility, traffic loads, and their channel access parameters. AI-/ML-based algorithms can be instrumental to learn the optimal operation under such dynamics, however, they need a proper characterization of the state of the wireless channel that capture these dynamics. The SF profile can be used to provide this characterization.

**Definition 1.** Let  $L = \{l_1, l_2, \cdots, l_{N_r}\}$  be the set of  $N_r$  thresholds of received signal strength sorted in ascending order. Let  $\xi_{n,i} = \{1: y(n) \in [l_i, l_{i+1})\}$  be indicator function of received signal being at the signal level  $[l_i, l_{i+1})$  at time n. Let  $N_m$  be the number of time slots over which we monitor the received signal strength. The SF profile  $S = \langle s_1, s_2 \cdots, s_{N_r} \rangle$  is the normalized histogram of the received signal strengths that are captured over a duration of  $N_m$  time slots, where:

$$s_{i} = \frac{\tilde{s}_{i}}{\sum_{j=1}^{N_{r}} \tilde{s}_{j}}, \text{ and } \tilde{s}_{k} = \sum_{n=1}^{N_{m}} \xi_{n,k}$$
 (3)

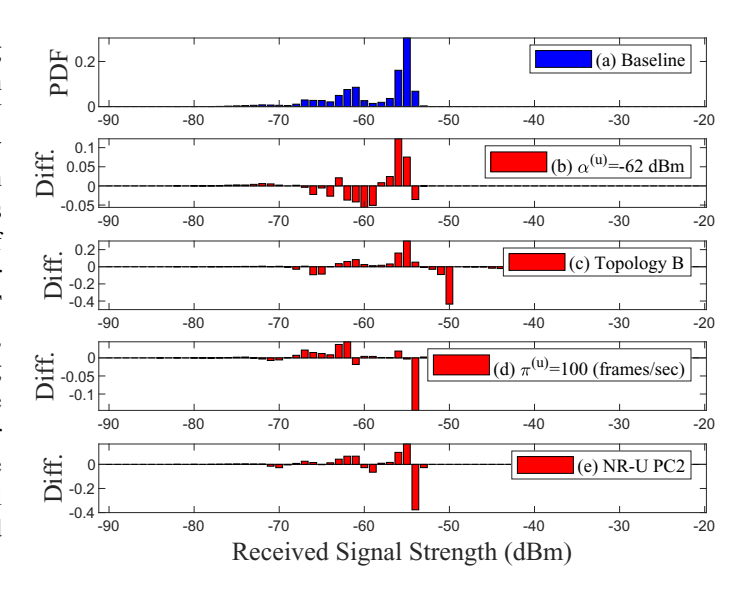


Fig. 3. (a) SF profile captured by an arbitrary Wi-Fi STA under the baseline scenario with Topology A,  $\alpha^{(u)} = -72$  dBm,  $\pi^{(u)} = 50$  frames/sec, and NR-U LBT with PC1; the difference between the SF profile captured under the the baseline scenario and SF profile captured when (b) ST of NR-U is changed to  $\alpha^{(u)} = -62$  dBm, (c) topology changes, and (d) LBT priority class of NR-U is changed to PC 2.

We next study the effectiveness of SF profile in tracking key network dynamics.

# A. Track Network Dynamics Using SF Profile

To study the feasibility of using SF profile to track NR-U and Wi-Fi network dynamics, we conducted system-level-based experiments in which we consider a baseline scenario with a fixed topology, and then apply changes to topology, traffic loads, and channel access parameters. We initially set the STs of NR-U and Wi-Fi to their standard settings, i.e.,  $\alpha^{(u)}=-72$  dBm and  $\alpha^{(w)}=-62$  dBm, respectively. The traffic intensity is set to  $\pi^{(u)}=50$  and  $\pi^{(w)}=50$  frames per second. NR-U and Wi-Fi networks contend with their highest LBT priority class (PC), i.e., PC 1, in which  $W_{\min}^{(u)}=4$ ,  $W_{\max}^{(u)}=8$ , and  $\rho^{(u)}=24$  microseconds, and their Wi-Fi counterparts are set to  $W_{\min}^{(w)}=4$ ,  $W_{\max}^{(w)}=8$ , and  $\rho^{(w)}=34$  microseconds, respectively. The SF profile constructed by an

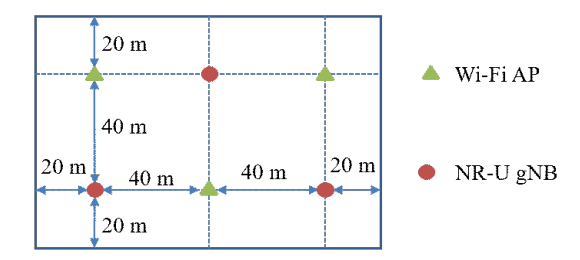


Fig. 4. Indoor simulation topology adopted by 3GPP 5G NR-U committee [8].

arbitrary (tagged) Wi-Fi device under the baseline scenario over a monitoring time of 5 seconds is plotted in Figure 3(a).

To study the effectiveness of the SF profile to track changes in ST setting, we change the STs for NR-U devices to -62 dBm and plot the difference between the baseline and updated SF profiles, as shown in Figure 3(b). The increase in the ST of NR-U devices triggers them to aggressively access the channel, which results in an increase of the density for some signal levels. This also forces other Wi-Fi devices to backoff for longer duration, resulting in a reduction of the density of their transmissions. To study the impact of mobility, we let all UEs and STAs, except the tagged Wi-Fi device, change their location (i.e., Topology B). The updated SF profile is plotted in Figure 3(c). As can be observed, mobility can cause significant change in the shape of SF profile and density of signal levels.

We increase the traffic intensity of NR-U networks to  $\pi^{(u)} = 100$  frames per second, and plot the difference between the baseline and the updated SF profiles in Figure 3(d). The density of the SF profile has been changed. We also evaluate the effectiveness of SF profile to capture changes in LBT parameters. We let NR-U network contend with PC 2, in which  $W_{\min}^{(u)}=8$  and  $W_{\max}^{(u)}=16$ . We observe some changes in the density of some signals levels. These observations reveal the effectiveness of the SF profile to be used for tracking and monitoring vital network dynamics, and thus, it can be considered as a powerful tool for AI-/ML-based algorithms that are developed to optimize the harmonious coexistence between NR-U and Wi-Fi networks. We still need a quantitative measure to value changes in the SF profile. These quantitative measures can also help in defining rules to decide on whether different dynamics require adapting any network parameters or not. We next provide some of these quantitative measures.

#### B. Measuring Divergence in SF Profile

We discuss some of the statistical similarity metrics that can be used to track changes happening in coexisting networks. We consider two arbitrary SF profiles that are captured over two different time duration, i.e, S and Q. Let  $D_{(\eta)}(S||Q)$  be the metric for measuring the difference between SF profiles S and Q based on the criterion  $\eta$ . We consider the following criteria:

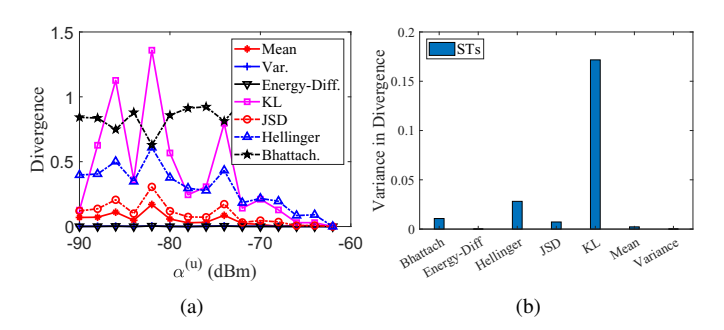


Fig. 5. (a) Divergence versus NR-U ST (last entry in the x-axis corresponds to the baseline case), and (b) variance of divergence under ST dynamics.

• Normalized difference in mean  $D_{(m)}(S||Q)$ :

$$D_{(m)}(S||Q) \doteq \frac{1}{l_{N_r} - l_1} |\text{mean}(S) - \text{mean}(Q)|$$
 (4)

• Normalized difference in variance  $D_{(v)}(S||Q)$ :

$$D_{(v)}(S||Q) \doteq \frac{1}{l_{N_r} - l_1} |\text{var}(S) - \text{var}(Q)|$$
 (5)

• Difference in energy  $D_{(q)}(S||Q)$ :

$$D_{(g)}(S||Q) \doteq \sum_{k=1}^{N_r} ||s_k - q_k||_2 \tag{6}$$

• Kullback-Leibler (KL) divergence measure  $D_{(KL)}(S||Q)$  [10]:

$$D_{(KL)}(S||Q) \doteq \sum_{k=1}^{N_r} s_k \log(s_k/q_k)$$
 (7)

• Jensen-Shannon divergence (JSD) measure  $D_{(JSD)}(S||Q)$  [11]:

$$D_{(JSD)}(S||Q) \doteq \frac{1}{2} D_{(KL)}(S||M) + \frac{1}{2} D_{(KL)}(Q||M),$$
where  $M = 0.5(S+Q)$  (8)

• Hellinger distance  $D_{(H)}(S||Q)$ :

$$D_{(H)}(S||Q) \doteq \frac{1}{\sqrt{2}} \sqrt{\sum_{k}^{N_r} (\sqrt{s_k} - \sqrt{q_k})^2}$$
 (9)

• Bhattacharyya distance  $D_{(B)}(S||Q)$  [10]:

$$D_{(B)}(S||Q) \doteq \sum_{k}^{N_r} \sqrt{s_k q_k} \tag{10}$$

The best metric for tracking network dynamics is the one that provides the highest variance. We next conduct simulation-based study to investigate the variance of these metrics under different dynamics in coexisting networks.

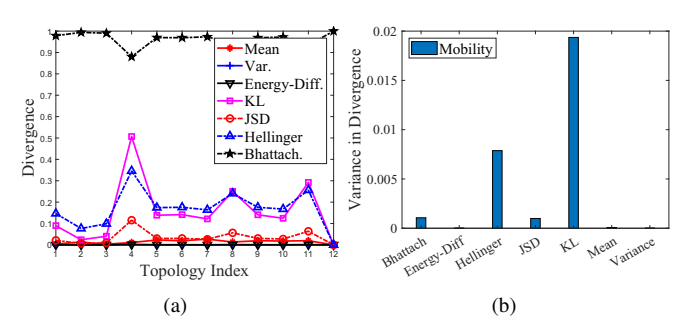


Fig. 6. Divergence versus topology index (last entry in the x-axis corresponds to the baseline case), and (b) variance of divergence under mobility dynamics.

#### VI. EVALUATION AND DISCUSSION

We develop a C++-based discrete-event system-level simulator to study the NR-U and Wi-Fi coexistence. Our simulation setup, traffic model, channel model, and LBT parameters are in line with those listed by 3GPP (see Annex A [2] [8]). We consider the indoor topology adopted by the 3GPP standardization committee, as shown in Figure 4. Every Wi-Fi AP serves five STAs and each NR-U gNB serves 5 UEs. Our simulator runs multi-threaded processes that work in parallel and simulate traffic generation, mobility, channel access procedures, i.e., EDCA and CAT4-LBT, of Wi-Fi and NR-U systems.

We evaluate the change in SF profiles captured by an arbitrary Wi-Fi device (tagged device) under different scenarios. We consider a baseline scenario, and let NR-U devices deviate from this baseline scenario. We evaluate the divergence between the SF profile captured in the baseline scenario and the SF profiles captured under different NR-U dynamics, as shown in Figures 5, 6, 7, and 8. We plot the metrics that we discussed in Section V-B versus the different factors. In plots of Figures 5(a), 6(a), 7(a), and 8(a), we consider the last entry of the x-axis to be the baseline scenario that we evaluate changes against. In bar plots of Figures 5(b), 6(b), 7(b), and 8(b), we show the variance for each divergence metric under different dynamics. These plots provide us good understanding on how dynamics of STs, mobility, traffic loads, and LBT PCs of NR-U network affect the shape and statistics of the SF profile. We are interested in investigating the effectiveness of the SF profile to track these dynamics, and whether the SF profile can be a good feature to be considered in the feature extraction/selection blocks shown in Figure 1. It also helps us select the best metric that suites the dynamic factor of interest.

In Figure 5(a), we plot the divergence between SF profiles captured by tagged Wi-Fi device versus the ST values used by NR-U devices. We observe that changing STs used by NR-U devices imposes high change in the SF profiles captured by the tagged Wi-Fi device. The KL divergence measure and Hellinger distance are the best metrics for characterizing this change because they have high variance, as shown in Figure 5(b). In Figure 6(a), we plot the divergence versus the topology index. We change the topology by letting NR-U and Wi-Fi devices move in a random-walk mobility pattern. We notice that different metrics express different divergence values under

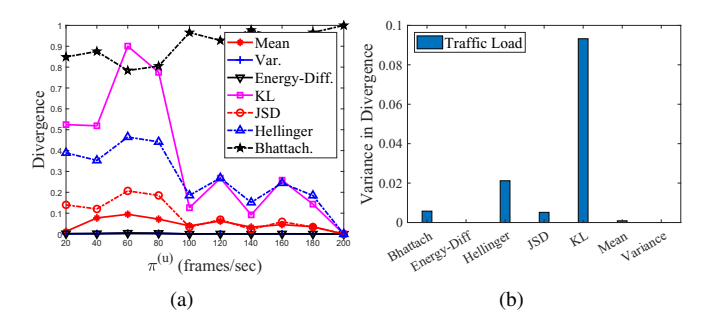


Fig. 7. Divergence versus NR-U traffic load (last entry in the x-axis corresponds to the baseline case), and (b) variance of the divergence under traffic dynamics.

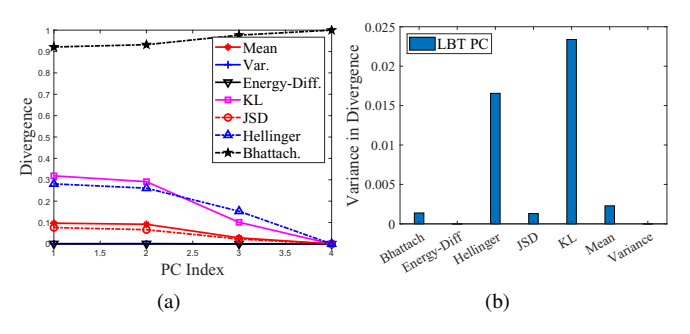


Fig. 8. Divergence versus NR-U PCs (last entry in the x-axis corresponds to the baseline case), and (b) variance of the divergence measures under LBT dynamics.

mobility, and the KL and Hellinger are the best metrics to characterize mobility dynamics, as shown in Figure 6(b). In Figure 7(a), we plot divergence between SF profiles versus the traffic load of the NR-U network. The change in NR-U traffic load imposes variation in the divergence values, and the KL and Hellinger distance are again the best metrics to indicate dynamics in traffic loads, as shown in Figure 7(b). In Figure 8(a), we plot divergence between SF profiles versus the index of the PC adopted by NR-U network (see Table 15.1.1-1 in [5] for their  $W_{\min}^{(u)}$ ,  $W_{\max}^{(u)}$ , and  $\rho^{(u)}$  values). We notice that changing LBT parameters impose different changes in the SF profile, and the KL and Hellinger are the best metrics to represent this change, as shown in Figure 8(b).

#### VII. RELATED WORK

Previous works on NR-U operation can be found in [12], [13], [14], [15]. Bayhan et al. [16] discussed the role of AI and ML in achieving harmonious LAA/Wi-Fi coexistence. Li *et al.* [17] proposed an ad-hoc-based framework for adapting STs used by LAA devices based on monitoring collision rates experienced by LAA devices. Iqbal *et al.* [18] conducted system-level simulations to study the setting of STs for LAA and Wi-Fi devices, and found that lowering Wi-Fi ST could potentially improve the throughput of LAA and Wi-Fi networks. Hirzallah *et al.* proposed AI-based frameworks for reducing collisions and improving throughput of full-duplex-enabled Wi-Fi network when coexisting with duty-cycle-based LTE system [19] and half-duplex-enabled Wi-Fi users [20]. Ajami

et al. [9] presented a stochastic geometry based analysis to analyze the coexistence between LTE and Wi-Fi systems, and recommended that Wi-Fi ST need to be adapted to achieve harmonious LAA/Wi-Fi coexistence. Authors in [21] proposed an online learning algorithm based on graph coloring evolution to allocate frequency and network resources among operators running NR-U service. Haider et al. [22] introduced a Qlearning based approach for selecting the backoff duration of LAA devices in which fairness with Wi-Fi systems can be guaranteed. Authors in [23] introduced a Q-learning based approach for controlling the channel occupancy time for LAA and muting LAA transmission overtime in order to improve the fairness with Wi-Fi systems. To facilitate research and evaluation of ML techniques in cross-technology coexistence. authors in [24] developed a framework in Linux OS. Song et al. [25] presented a cooperative LBT and multi-user zero forcing interference cancellation framework to reduce collision rates in NR-U/Wi-Fi coexistence. Authors in [26] introduced a queuing model to characterize different strategies for splitting NR-U traffic between millimeter and sub-6 GHz unlicensed bands. Yang et al. [27] proposed a fuzzy Q-learning based algorithm to improve the time alignment of sensing slots between LAA and Wi-Fi systems. Authors in [28] proposed a chaotic Q-learning algorithm to adapt contention window in LTE/Wi-Fi coexistence.

#### VIII. CONCLUSION

In this work, we introduced the concept of SF profile for modeling the state of unlicensed channel when it hosts heterogeneous coexisting technologies, such as 5G NR-U and Wi-Fi. We showed that the SF profile can be used to track vital changes happening in coexisting networks by computing the changes in SF profiles captured overtime. AI-/ML-based algorithms can utilize the SF profile to model and track the state of the wireless environment when they adapt key channel access parameters for NR-U and Wi-Fi networks. The Kullback-Leibler divergence measure and Hellinger distance are the best metrics to be used to signal changes of different network dynamics, including changes in ST values, LBT parameters, traffic loads, and mobility.

# REFERENCES

- [1] IEEE, "IEEE-part 11: Wireless LAN medium access control (MAC) and physical layer (PHY) specifications-amendment 4," http://ieeexplore.ieee.org/servlet/opac?punumber=6687185, 2013.
- [2] 3GPP, "Study on licensed-assisted access to unlicensed spectrum," 3GPP TR. 36.889 v13.0.0., Jun. 2015.
- [3] —, "Study on NR-based access to unlicensed spectrum," no. 3GPP TR 38.889 v16.0.0, Dec. 2018.
- [4] M. Hirzallah, M. Krunz, and Y. Xiao, "Harmonious cross-technology coexistence with heterogeneous traffic in unlicensed bands: Analysis and approximations," *IEEE Transactions on Cognitive Communications* and Networking, vol. 5, no. 3, pp. 690–701, Sep. 2019.
- [5] 3GPP, "Physical layer procedures," 3GPP TR. 36.213 v15.1.0., Mar. 2018.
- [6] IEEE, "IEEE-part 11: Wireless LAN MAC and PHY layer specifications," pp. 1–3534, 2016.
- [7] D. López-Pérez, A. Garcia-Rodriguez, L. Galati-Giordano, M. Kasslin, and K. Doppler, "IEEE 802.11 be extremely high throughput: The next generation of wi-fi technology beyond 802.11 ax," arXiv preprint arXiv:1902.04320, 2019.

- [8] 3GPP, "Study on NR-based access to unlicensed spectrum," no. 3GPP TR 38.889 v16.0.0, Dec. 2018.
- [9] A. Ajami and H. Artail, "On the modeling and analysis of uplink and downlink IEEE 802.11ax Wi-Fi with LTE in unlicensed spectrum," *IEEE Transactions on Wireless Communications*, vol. 16, no. 9, pp. 5779–5795, Sep. 2017.
- [10] S. M. Ali and S. D. Silvey, "A general class of coefficients of divergence of one distribution from another," *Journal of the Royal Statistical Society: Series B (Methodological)*, vol. 28, no. 1, pp. 131–142, 1966.
- [11] F. Nielsen, "A family of statistical symmetric divergences based on jensen's inequality," arXiv preprint arXiv:1009.4004, 2010.
- [12] E. Semaan, J. Ansari, G. Li, E. Tejedor, and H. Wiemann, "An outlook on the unlicensed operation aspects of NR," in *Proc. of IEEE Wireless Communications and Networking Conference (WCNC'17)*, March 2017, pp. 1–6.
- [13] E. Pateromichelakis, O. Bulakci, C. Peng, J. Zhang, and Y. Xia, "LAA as a key enabler in slice-aware 5G RAN: Challenges and opportunities," IEEE Communications Standards Magazine, vol. 2, no. 1, pp. 29–35, MARCH 2018.
- [14] S. Lagen, L. Giupponi, S. Goyal, N. Patriciello, B. Bojovic, A. Demir, M. Beluri, and J. Mangues-Bafalluy, "New radio beam-based access to unlicensed spectrum: Design challenges and solutions," arXiv preprint arXiv:1809.10443, 2018.
- [15] Y. Huo, X. Dong, W. Xu, and M. Yuen, "Enabling multi-functional 5g and beyond user equipment: A survey and tutorial," *IEEE Access*, vol. 7, pp. 116 975–117 008, 2019.
- [16] S. Bayhan, G. Gür, and A. Zubow, "The future is unlicensed: Coexistence in the unlicensed spectrum for 5G," arXiv preprint arXiv:1801.04964, 2018.
- [17] L. Li, J. P. Seymour, L. J. Cimini, and C. Shen, "Coexistence of Wi-Fi and LAA networks with adaptive energy detection," *IEEE Transactions* on Vehicular Technology, vol. 66, no. 11, pp. 10384–10393, Nov 2017.
- [18] M. Iqbal, C. Rochman, V. Sathya, and M. Ghosh, "Impact of changing energy detection thresholds on fair coexistence of Wi-Fi and LTE in the unlicensed spectrum," in 2017 Wireless Telecommunications Symposium (WTS), April 2017, pp. 1–9.
- [19] M. Hirzallah, W. Afifi, and M. Krunz, "Full-duplex-based rate/mode adaptation strategies for Wi-Fi/LTE-U coexistence: A POMDP approach," *IEEE Journal on Selected Areas in Communications*, vol. 35, no. 1, pp. 20–29, Jan 2017.
- [20] M. Hirzallah, W. Afifi, and M. Krunz, "Provisioning qos in wi-fi systems with asymmetric full-duplex communications," *IEEE Transactions on Cognitive Communications and Networking*, vol. 4, no. 4, pp. 942–953, Dec 2018.
- [21] M. Hirzallah, Y. Xiao, and M. Krunz, "Matchmaker: An inter-operator network sharing framework in unlicensed bands," in proc. of IEEE International Conference on Sensing, Communication, and Networking (SECON), June 2019, pp. 1–9.
- [22] M. Haider and M. Erol-Kantarci, "Enhanced lbt mechanism for Iteunlicensed using reinforcement learning," in *IEEE Canadian Conference* on Electrical Computer Engineering (CCECE), May 2018, pp. 1–4.
- [23] V. Maglogiannis, D. Naudts, A. Shahid, and I. Moerman, "A q-learning scheme for fair coexistence between lte and wi-fi in unlicensed spectrum," *IEEE Access*, vol. 6, pp. 27278–27293, 2018.
- [24] F. A. P. De Figueiredo, X. Jiao, W. Liu, R. Mennes, I. Jabandi, and I. Moerman, "A spectrum sharing framework for intelligent next generation wireless networks," *IEEE Access*, vol. 6, pp. 60704–60735, 2018.
- [25] H. Song, Q. Cui, Y. Gu, G. L. Stber, Y. Li, Z. Fei, and C. Guo, "Cooperative lbt design and effective capacity analysis for 5g nr ultra dense networks in unlicensed spectrum," *IEEE Access*, vol. 7, pp. 50 265–50 279, 2019.
- [26] X. Lu, E. Sopin, V. Petrov, O. Galinina, D. Moltchanov, K. Ageev, S. Andreev, Y. Koucheryavy, K. Samouylov, and M. Dohler, "Integrated use of licensed- and unlicensed-band mmwave radio technology in 5g and beyond," *IEEE Access*, vol. 7, pp. 24376–24391, 2019.
- [27] C. S. Yang, C. K. Kim, J. Moon, S. Park, and C. G. Kang, "Channel access scheme with alignment reference interval adaptation (aria) for frequency reuse in unlicensed band Ite: Fuzzy q-learning approach," *IEEE Access*, vol. 6, pp. 26438–26451, 2018.
- [28] E. Pei, J. Jiang, L. Liu, Y. Li, and Z. Zhang, "A chaotic q-learning based licensed assisted access scheme over the unlicensed spectrum," *IEEE Transactions on Vehicular Technology*, pp. 1–12, 2019.